

# Short-term frequency stability analysis of time-keeping $^{87}\text{Rb}$ fountain clock at NTSC

Hui Zhang<sup>1,2</sup>, Sichen Fan<sup>1,2</sup>, Jiang Chen<sup>1,2\*</sup>, Dandan Liu<sup>1,2</sup>, Yong Guan<sup>1,2</sup>, Yang Bai<sup>1,2</sup>, Jun Ruan<sup>1,2\*</sup>, Shougang Zhang<sup>1,2</sup>

<sup>1</sup>National Time Service Center, Chinese Academy of Sciences/Xi'an/China

<sup>2</sup>Key Laboratory of Time Reference and Application, Chinese Academy of Sciences/ Xi'an /China

Email: zhanghui1094@ntsc.ac.cn, \*chenjiang@ntsc.ac.cn, \*ruanjuan@ntsc.ac.cn

**Abstract**—Frequency stability is one of the most critical metrics for time-keeping atomic clocks. This paper analyses the effects of various noises on the short-term frequency stability of the time-keeping  $^{87}\text{Rb}$  fountain clock developed by the National Time Service Center, Chinese Academy of Sciences, identifies the main noise sources, and gives suggestions for improvement.

**Keywords**—time-keeping  $^{87}\text{Rb}$  fountain clock, short-term frequency stability, quantum projection noise, local oscillator phase noise,

## I. INTRODUCTION

Due to their excellent frequency stability, time-keeping  $^{87}\text{Rb}$  fountain clocks are key devices in modern time-keeping systems [1,2,3]. Its short-term frequency stability is mainly determined by quantum projection noise (QPN) [4], electronic detection noise (EDN), laser detection noise (LDN) [5], and local oscillator (LO) phase noise [6].

This paper evaluates the effects of these noises on the short-term frequency stability of a time-keeping  $^{87}\text{Rb}$  fountain clock developed by the National Time Service Centre (NTSC), Chinese Academy of Sciences, identifies the main sources of noise, and suggests improvements.

## II. ANALYSIS AND ESTIMATION

According to [7], the formula for the short-term frequency stability (SFS) of the clock is

$$\sigma_y(\tau) = \frac{1}{\pi Q_{at}} \frac{\sigma_{\delta P}}{P} \sqrt{\frac{T_c}{\tau}} = \frac{1}{\pi Q_{at}} \left( \frac{1}{N_{det}} + \frac{2\sigma_{\delta N}^2}{N_{det}^2} + \gamma_{laser}^2 + \gamma_{LO}^2 \right) \sqrt{\frac{T_c}{\tau}} \quad (1)$$

where  $Q_{at}$  represents the quality factor of the atomic discriminant curve,  $\sigma_{\delta P}$  represents atomic transition probability fluctuation variance (ATPFV),  $P$  equal to  $1/2$ ,  $T_c$  represents one clock cycle,  $\tau$  represents integration time,  $N_{det}$  represents atomic number arriving at detection zone,  $\frac{1}{N_{det}}$  represents QPN,  $\frac{2\sigma_{\delta N}^2}{N_{det}^2}$  represents EDN,  $\gamma_{laser}^2$  represents LDN,  $\gamma_{LO}^2$  represents the effect of the LO phase noise through the Dick effect. (2) can be obtained from (1).

$$\sigma_{\delta P}^2 = P^2 \left( \frac{1}{N_{det}} + \frac{2\sigma_{\delta N}^2}{N_{det}^2} + \gamma_{laser}^2 + \gamma_{LO}^2 \right) \quad (2)$$

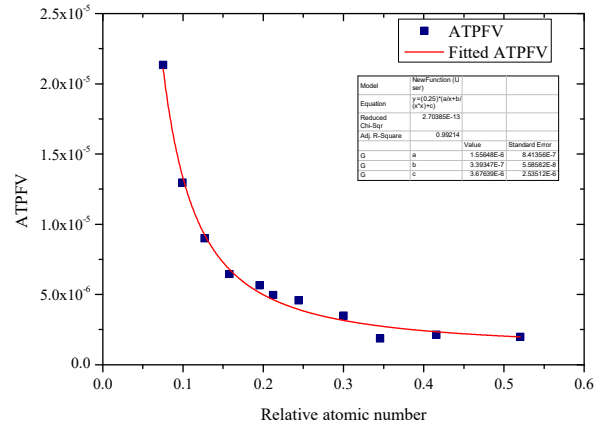


Fig. 1. Variation in ATPFV with atomic number.

By measuring the atomic transition probability at different atomic number, a curve of ATPFV as a function of the atomic number is fitted to (2). Based on the relevant parameters of the curve, the effects of the above-mentioned noises on ATPFV can be obtained respectively, and then the effect of each noise on the SFS is estimated according to (1). The different atomic number is achieved by changing the input power of the state-selection cavity. The ATPFV is calculated from the atomic transition probability of 400 measurements at the center frequency of the Ramsey fringe deviating from 0.5 Hz. Fig. 1 shows ATPFV for different atomic numbers.

We use the function  $y = 0.25 \times (a/x + b/x^2 + c)$  to perform curve fitting on the above values, and obtain  $a = (1.56 \pm 0.84) \times 10^{-6}$ ,  $b = (0.34 \pm 0.058) \times 10^{-6}$ ,  $c = (3.68 \pm 2.54) \times 10^{-6}$ .

With parameter  $a$ , the maximum atomic number reaching the detection zone can be estimated from equation (3),

$$\frac{a}{K \times N_{det}} = \frac{1}{N_{det}} \quad (3)$$

where  $K$  is the proportional coefficient between the relative and the actual atomic number, and  $K = 1.56 \times 10^{-6}$ , and  $N_{det} = 3.33 \times 10^5$  (a relative value of 0.52). The effect of QPN on our clock SFS is  $1.39 \times 10^{-13} \tau^{1/2}$ , that of EDN is estimated to be  $9.02 \times 10^{-14} \tau^{1/2}$  using parameter  $b$ . With parameter  $c$ , the effect of the LO phase noise on is estimated to be  $1.54 \times 10^{-13} \tau^{1/2}$ . Since the effect of LDN is much smaller than that of

LO phase noise, the parameter  $c$  is used to estimate the effect of the LO phase noise.

The effect of LDN estimation process is as follows:

$$\sigma_{\delta P-LDN}^2 = \int_0^\infty S_{\delta\gamma}(f) |H(f)|^2 df \quad (4)$$

where  $\sigma_{\delta P-LDN}^2$  represents LDN-induced ATPFV,  $S_{\delta\gamma}(f)$  represents the power spectral density of the spontaneous emission rate fluctuation,  $H(f)$  represents the equivalent filter function of the detection system [8].

$$S_{\delta\gamma}(f) = \left(\frac{2\omega_{laser}}{\Gamma}\right)^2 S_y(f) + S_{\delta I/I}(f) \quad (5)$$

where  $S_y(f)$  and  $S_{\delta I/I}(f)$  represent the relative frequency noise and intensity noise of detection laser, respectively, and  $\omega_{laser}$  is the wavelength of detection laser.

$$H(f) = \frac{1}{4} e^{-\pi^2 f^2 t_w^2} (1 - e^{-i2\pi f \Delta t}) \quad (6)$$

where  $t_w$  represents the half-width (1/e) of the time of flight (TOF) signal generated by detecting the atomic number at  $|5^2S_{1/2}, F=2, m_F=0\rangle$  or  $|5^2S_{1/2}, F=1, m_F=0\rangle$ , and  $\Delta t$  represents the time interval between TOF signals.

Based on the relative frequency and intensity noise of the detection laser measured in Fig. 2 and Fig. 3 and the

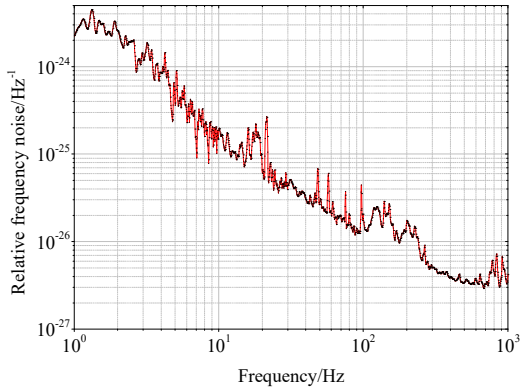


Fig. 2. Relative frequency noise of detection laser.

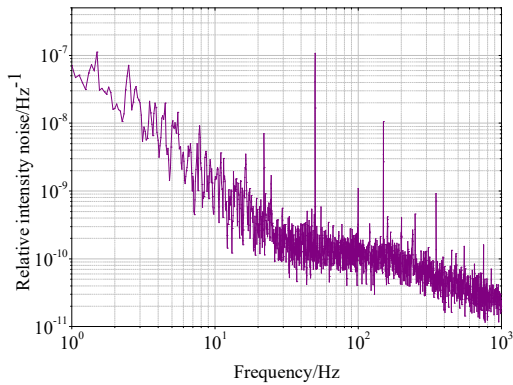


Fig. 3. Relative intensity noise of detection laser.

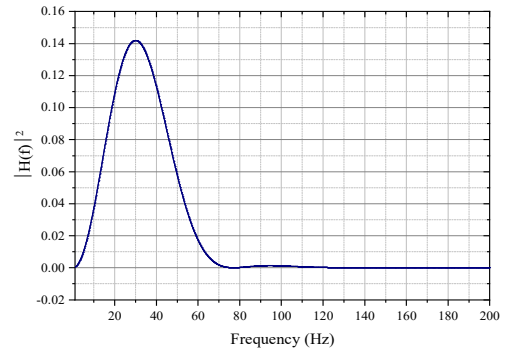


Fig. 4. Filter function.

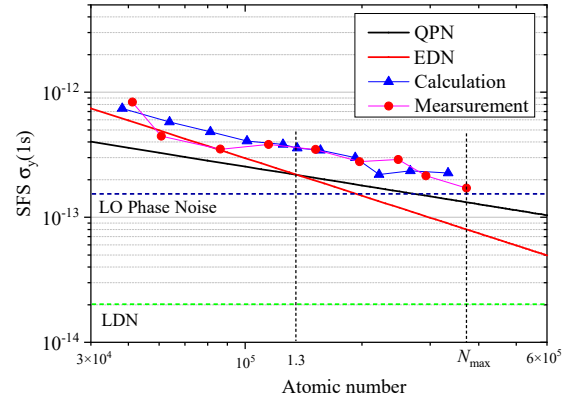


Fig. 5. Variation of the clock frequency stability (1s) with atomic number.

$|H(f)|^2$  for our clock in the Fig. 4, the effect of LDN on our clock SFS was calculated using (4)-(6) as  $2.03 \times 10^{-14} \tau^{1/2}$ .

### III. DISCUSSION

Calculated and measured SFS with different atomic number, and fitted parameters  $a$ ,  $b$ ,  $c$ , the effect of the different noise terms on the 1 s stability of the clock is obtained as shown in Fig. 5.

As can be seen in Fig. 5, the SFS of the clock decreases with the increase of the number of atoms. When the atomic number is less than  $1.3 \times 10^5$ , the noise sources affecting the SFS of the clock are QPN and EDN, and when the number of atoms is greater than  $1.3 \times 10^5$ , QPN and LO phase noise gradually dominate as the number of atoms increases.

The effect of QPN can be suppressed by increasing the number of captured atoms in the MOT zone, for example by using the 2D-MOT technique [9]. In addition to shortening the “dead time”, the effect of LO phase noise can be reduced by applying a lower phase noise oscillator, such as a cryogenic sapphire oscillator (CSO) [10] or an optically stabilization microwave oscillator (OSMO) [11].

### IV. CONCLUSIONS

This article describes the SFS analysis of the time-keeping  $^{87}\text{Rb}$  fountain clock developed by the NTSC, the effect of QPN on the SFS of the clock is  $1.39 \times 10^{-13} \tau^{1/2}$ , that of LO phase noise through the Dick effect is  $1.53 \times 10^{-13} \tau^{1/2}$ , that of EDN is  $9.04 \times 10^{-14} \tau^{1/2}$ , and that of LDN is  $2.03 \times 10^{-14} \tau^{1/2}$ . The SFS (1s) of the clock is currently  $1.71 \times 10^{-13}$ , and the main source of noise is the QPN and the LO phase noise,

and the subsequent technical solutions to improve the short-term frequency stability of the clock.

#### REFERENCES

- [1] S. Peil, T. B. Swanson, J. Hanssen etc “Microwave-clock timescale with instability on order of  $10^{-17}$ ,” *Metrologia*, vol. 54, pp. 247-252, March 2017.
- [2] I. Blinov, A. Boiko, N. Kosheliaevskii etc “First Experiments on application of Rb fountain frequency standards for TA SU time scale maintenance,” *Proc. Of 2018 European Frequency and Time Forum*, pp. 17933454, April 2018.
- [3] H. Zhang, J. Ruan ,D. D. Liu etc “Development and preliminary operation of  $^{87}\text{Rb}$  continuously running atomic fountain clock at NTSC,” *IEEE Trans. Instrum. Meas.* vol. 71, pp. 1008312, November 2022.
- [4] G. Santarelli, P. Laurent, P. Lemonde etc “Quantum projection noise in an atomic fountain: A high stability cesium frequency standard,” *Phys. Rev. Lett.* vol. 82, pp. 4619-4622 1999.
- [5] S. Lee, M. S. Heo, T. Y. Kwon etc “Operating atomic fountain clock using robust DBR laser:short-term stability analysis,” *IEEE Trans. Instrum. Meas.* vol. 66, pp. 1349-1354, June 2017.
- [6] G. J. Dick, “Local oscillator induced instabilities in trapped ion frequency standards,” *Proc. of 19th Precise Time and Time Interval Applications and Planning Meeting*, pp.1-3, Dec 1987.
- [7] M. Abgrall, “Evaluation des performances de la fontaine atomique PHARAO, participation à l’étude de l’horloge spatiale PHARAO”, Univ. Pierre et Marie Curie-Paris VI, France, 2003.
- [8] T. Leveque, B. Faure, F. Esnault X, etc. “PHARAO laser source flight model: Design and performances”, *Rev. Sci. Instrum.* vol. 86, pp.033104, 2015
- [9] C. J. Wu, J. Ruan, J. Chen, etc. “A two-dimensional magneto-optical trap for a cesium fountain clock”, *Acta Phys. Sin.* vol.62, pp.063201, 2013.
- [10] Fluhr, C.; Grop, S.; Dubois, B.; Kersalé, Y.; Rubiola, E.; Giordano, V. Characterization of the individual short –term frequency of Cryogenic Sapphire Oscillators at the  $10^{-16}$ . *IEEE Trans. Ultrason. Ferroelectr. Freq.Control.* 63, 915-921, 2016.
- [11] B. Lipphardt, V. Gerginov, S. Weyers etc. “Optical stabilization of a microwave oscillator for fountain clock interrogation.” *IEEE Trans. Ultrason. Ferroelectr. Freq. Control.* vol.64, 761-766, 2017.